# Screening and Optimal Design of CCU Processes using Superstructure Optimization

Flemming Holtorf, B.Sc.[a], Luise Bering, B.Sc.[a], Andreas Vellguth, B.Sc.[a], Daniel Felder, B.Sc.[a], Pascal Padberg, B.Sc.[a]

[a] *Aachener Verfahrenstechnik - Process Systems Engineering, RWTH Aachen University, Aachen, Germany*

**Abstract**

Algal biomass production, mineralization, and chemical conversion as promising carbon dioxide utilization processes are compared with regard to economic as well as environmental factors. The production of the chemicals methanol, dimethyl ether, and dimethyl carbonate is selected as the most viable alternative among all options. The integrated production of the proposed chemicals is evaluated for a wide range of trade-offs between economic potential and environmental impact by applying multi-objective superstructure optimization. The results indicate that direct hydrogenation of $CO_2$ to methanol with subsequent dehydration to dimethyl ether is on the verge of profitability (including capture cost) while achieving a positive net $CO_2$ consumption of ca. 68 % of supplied $CO_2$ when direct and indirect emissions are accounted for; and 85 % when only direct emissions are considered.

## 1. Introduction

To mitigate the effects of ever increasing carbon dioxide emissions, policy makers around the world are implementing $CO_2$ reduction schemes. The European Union alone is targeting a 40 % cut in emissions by 2030 compared to 1990 [1]. While renewable energy sources like wind or solar power will play an important part, their intermittent nature and high cost dictate their supplementation by flexible and independent power sources.

Traditionally, Germany's coal power plants carry the base load on the national power grid; consequently they are among the top $CO_2$ emitters in Europe. To continue operating the existing and proven infrastructure and simultaneously cut $CO_2$ emissions, separation and sequestration of exhaust carbon dioxide is widely considered [2–4]. Although carbon capture and storage (CCS) is less expensive than for example wind or solar power, it comes with an economic penalty compared to conventional power generation. Additionally, concerns among the population over onshore underground storage of $CO_2$ continue to hinder its implementation [5, 6].

Carbon capture and utilization (CCU) offers the potential to reuse $CO_2$ as a feedstock for several processes. That way, $CO_2$ emission to the atmosphere is delayed depending on the final product and a life cycle of $CO_2$ is implemented [7]. Nevertheless, CCU can be expected to have a much smaller scale impact on carbon dioxide mitigation than CCS as the downstream markets for potential products are limited.

Several CCU processes [8] including mineral carbonation [9], algae farms [10], and the production of chemicals or fuels [11, 12] have been proposed over the years and shall be reviewed briefly before their evaluation in the following chapters.

Mineralization of $CO_2$ has been identified as a processes with the ability to store large volumes of $CO_2$ for an unlimited period of time [13]. Direct carbonation of magnesium silicate rock is the most straight forward process, but requires high $CO_2$ temperatures and pressures. Therefore, in modern processes $CO_2$ is neutralized in a reaction with activated forms of alkaline earth metals to form inert carbonates. The most commonly suggested feedstocks – magnesium and calcium – can be obtained in large quantities either from earth abundant olivine or serpentine rock, or precipitated from sea water [9, 14].

Åbo Akademi (ÅA) drives development on one of the most studied and straight forward processes [9, 15]. This process features solid-solid extraction of $MgSO_4$ with ammonium sulfate salts and decarbonation of flue gas with solid MgOH. The Nottingham process is a close competitor, that uses liquid phase extraction and carbonation, but requires more energy [9]. As an alternative Xie et al. [14] propose activation and precipitation of CaCl and MgCl-ions in sea water in an electrochemical cell. While this technology is promising, it is not far enough developed to be implemented at an industrial scale.

Algal biomass is a promising source for biodiesel in the near future that has been studied extensively [10, 18–20]. Generally, biological pathways of $CO_2$ utilization include the potential to reuse all $CO_2$ produced within the process leading to low direct greenhouse gas emission of the entire process [10]. Compared to other plants used for biodiesel production such as corn, rape, oil palm, and sugar beet, algae offer higher energy content and therefore a higher energy yield [18]. Other than the formerly listed plants, the cultivation of algae does not compete with the food industry, as algae can be cultivated at non-agricultural land

| Product | Reaction | No. |
|---|---|---|
| Syngas from Combined Reforming | | |
| Steam Methane Reforming (SMR) | $H_2O + CH_4 \longrightarrow 3\,H_2 + CO$ | (R1) |
| Water Gas Shift (WGS) | $H_2O + CO \longleftrightarrow H_2 + CO_2$ | (R2) |
| Dry Methane Reforming (DMR) | $CO_2 + CH_4 \longrightarrow 2\,H_2 + 2\,CO$ | (R3) |
| MeOH direct | $3\,H_2 + CO_2 \longrightarrow CH_3OH + H_2O$ | (R4) |
| MeOH via syngas | $2\,H_2 + CO \longrightarrow CH_3OH$ | (R5) |
| DME from MeOH | $2\,CH_3OH \longrightarrow CH_3OCH_3 + H_2O$ | (R6) |
| DME via syngas | $3\,H_2 + 3\,CO \longrightarrow CH_3OCH_3 + CO_2$ | (R7) |
| DMC | $CO_2 + C_2H_4O + 2\,CH_3OH \longrightarrow C_3H_6O_3 + C_2H_6O_2$ | (R8) |

Table 1: Chemical Production Routes [11, 16, 17]

[18]. There is a variety of different kinds of algae available that have varying lipid content, productivity and growth rate. Important effects on the algae growth and therefore the efficiency of the production are sunlight availability, temperature fluctuations, and harvest time [20].

Numerous chemical processes can utilize $CO_2$ as a carbon source. Novel approaches to existing processes and the production of novel chemicals allow additional $CO_2$ incorporation in the future. Some major process alternatives close to implementation with significant $CO_2$ consumption (listed in Table 1) fall into two categories:

- **Combined methane reforming (R1-3) with $CO_2$ and $H_2O$ to synthesis gas (syngas) includes both dry methane reforming (DMR) and steam methane reforming (SMR)**
  These processes require high operating temperatures, but are comparably compatible with existing infrastructure [21].

- **Direct synthesis of hydrocarbons from $CO_2$ and $H_2$**
  These processes can operate at lower temperatures, but have not achieved high yields yet. Additionally, hydrogen from renewable sources is still expensive [16].

In order to design an optimal CCU process, the three distinctly different alternatives (mineralization, biological, and chemical utilization) shall be reviewed in terms of their $CO_2$ utilization costs (Section 3) and evaluated based on a CCS reference case (Section 2). The most promising CCU option is then analyzed in further detail within the scope of a superstructure. In order to account for both environmental issues in terms of $CO_2$ emissions and economic viability, multi-objective optimization is applied to find the best process design (Section 5) [22]. In addition, social impact, controllability, and safety of the processes are briefly reviewed to allow a fair comparison to other proposals.

## 2. Reference Case: Carbon Capture and Storage

A reference case is introduced to allow an evaluation of different CCU processes with regard to costs based on state-of-the-art CCS technologies. Because the economic viability of certain CCS and CCU technologies can vary between different plant sites, a reference case needs to specify a particular location.

Several geological studies haven been undertaken to evaluate the $CO_2$ storage capacity in Europe and Germany [5, 23]. It was concluded that depleted oil and gas fields (DOGF) and saline aquifers (SA) are the most promising candidates; both can be found on- and offshore. Among these, large onshore DOGFs are the cheapest, but also the least available storage sites [24]. Nevertheless, the $CO_2$ storage capacity for Europe, and especially for Germany, might be highly overestimated even without taking additional restrictions like source-sink matching, acceptance issues [6] and injection rate constraints into account [5, 23].

Due to a large number of coal power plants, the German state of North Rhine-Westphalia (NRW) is considered one of the largest emitters of $CO_2$ in Europe [5]. Therefore, as a CCS reference case a coal power plant with post-combustion $CO_2$ capture in Lünen (NRW) operated by the STEAG GmbH is chosen [25]. This plant meets the common reference size of $500\,MW_{el}$ used for comparison among different CCS technologies [26, 27]. Furthermore, transport via pipeline and injection of the $CO_2$ into a depleted gas field (DGF) are chosen, because they account for the most feasible and furthest developed option [24]. The DGF can be found in North West Germany, about 250 km away from the plant in Lünen [5].

The costs for capturing $CO_2$, the transportation via pipeline from Lünen (NRW) to an on-shore DGF, and the injection into the DGF are estimated at $60\,€\,t^{-1}_{CO_2,captured}$ and consist of 8 € for transport, 10 € for underground injection and storage and 42 € for carbon capture [24, 26]. These overall costs of should be undercut by generating CCU processes.

## 3. CCU Process Types

For an weighted evaluation of the considered processes (mineralization, algae biomass and chemicals production) each process is graded on a scale from 1 to 5; 5 being the optimal process feature. The resulting grades are obtained by evaluating three distinctive criteria and multiplying them with their assigned weights. Lastly, the weighted grades are summed up to obtain the final validation score of each process. In this context, the following criteria are introduced:

- **Market size [0.5]**
  The market size is obtained by multiplying the worldwide production in $[t_{Product}]$ and the incorporated amount of $CO_2$ per tonne of product in $[t_{CO_2}\, t_{Product}^{-1}]$. This is further translated to the grading of 1 to 5.
- **Technical readiness [0.3]**
  **1** Conceptual design.
  **2** Lab scale experiments have been completed.
  **3** Integrated prototype has been developed.
  **4** Implemented at pilot plant scale.
  **5** Proven at industrial scale.
- **Environmental impact [0.2]**
  A grade of 5 is awarded to a process with no harmful emissions or by-products.

The weights have been chosen with the aim to select a CCU process, which primarily has a large potential to incorporate significant amounts of $CO_2$ (0.5) and is, in addition, technically viable in the short-term perspective (0.3). Also the environmental impact of the process should not countervail its positive impact on $CO_2$ emissions (0.2). It should be noted that the choice of weights has a large impact on the results.

To ensure comparability, each process is designed to utilize 20 % of the $CO_2$ emitted at the 500 $MW_{el}$ reference plant in Lünen [25], which is equivalent to a value of 75 $t_{CO_2}\, h^{-1}$. This amount is chosen with respect to a common plant scale for the production of chemicals.

### *3.1. Mineralization*

In the following, the ÅA process shown in Fig. 1 is considered. For simplicity serpentine is approximated as chrysotile ($Mg_3(Si_2O_5)(OH)_4$), its main component. The extraction is carried out with ammonium sulfate ($(NH_4)_2SO_4$) in a solid-solid reactor (reaction R9), that contains small amounts of water.

$$Mg_3(Si_2O_5)(OH)_4 + 3\,(NH_4)_2SO_4 \longrightarrow 3\,MgSO_4 + 2\,SiO_2 + 5\,H_2O + 6\,NH_3 \quad (R9)$$

After separating the gaseous ammonium from water, the sulfates (e.g. $MgSO_4$) are dissolved in water, and effectively separated from insoluble rock components (e.g. $SiO_2$). In solution, magnesium sulfates are reacted with $NH_3$ to form hydroxides and are precipitated at different pH-levels (reaction R10).

$$MgSO_4 + 2\,H_2O + 2\,NH_3 \longrightarrow Mg(OH)_2 + (NH_4)_2SO_4 \quad (R10)$$

The resulting hydroxides are highly reactive with $CO_2$ and form stable carbonates in the process (reaction R11). The high reactivity allows the process to operate directly on flue gas (20 $\%_{vol}$ $CO_2$), eliminating the costly carbon capture and purification step.

$$Mg(OH)_2 + CO_2 \longrightarrow MgCO_3 + H_2O \quad (R11)$$

Ammonium-sulfate is regenerated by crystallization / evaporation of the remaining solution.

In order to estimate the costs of a carbonation plant in Lünen, the following parameters are derived from Khoo et al. [28]:

- Mineral costs are 6.6 € $t^{-1}$
- 3.1 $t_{Mineral}\, t_{CO_2}^{-1}$ are required
- Mineral shipment costs $170 \times 10^{-6}$ € $t^{-1}\, km^{-1}$
- 0.5 $t_{CO_2}$ indirectly emitted for each captured $t_{CO_2}$

Energy costs are assumed to be 10 € $MW^{-1}\, h^{-1}$ [29, 30]. According to Zevenhoven [31] the energy requirements can be estimated at 5.9 GJ $t_{CO_2}^{-1}$ for the extraction process and 1.8 GJ $t_{CO_2}^{-1}$ for the ammonium sulfate recovery[1]. Serpentine minerals can be acquired from Donai, Portugal [32], resulting in a 3000 km shipping route. From these assumptions operating costs of 88 € $t_{CO_2}^{-1}$ are calculated. This price tag already includes indirect emissions. Disregarding indirect emissions a cost of 44 € $t_{CO_2}^{-1}$ is calculated.

Besides the cost of the process, the lack of saleable products[2] is the main drawback. For $MgCO_3$ no considerable markets exist, so that it can only be used for land reclamation so far [13]. As the operating cost per $t_{CO_2}$ is higher than for the CCS reference case, mineralization seems unsuitable to mitigate carbon capture cost. Additionally the lack of product opens the question to what extend mineralization can be considered sustainable carbon utilization [33].

Application of the process criteria to the ÅA process results in an average grade of 2 as shown in Figure 4. The process does not emit harmful substances to the environment and compensates its own $CO_2$ emissions, but mining and transportation of rock impact its environmental balance and award it a grade of 3 in the category "environment". The lack of saleable products makes the process fall behind to a grade of 1 in the category "market size". The feasibility of the ÅA process has been experimentally

[1] With vapour recovery.
[2] Production of lime as building material would require additional steps and re-release $CO_2$.

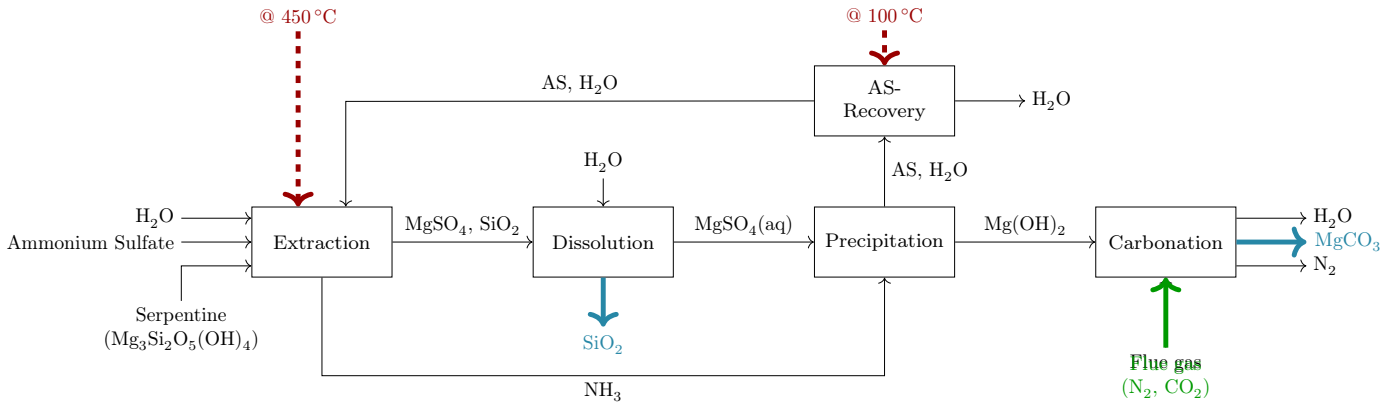


Figure 1: Åbo Akademi Carbonation Process (red: heat stream)

proven [34], process models have been developed and the pilot plant scale up is being prepared [35]. The process can thus be considered feasible and a technical application is in sight. This results in a grade of 3 for "technical readiness".

Over all, it can be concluded, that mineral carbonation is a viable alternative to CCS, especially where underground injection is impossible or unwanted, but it is not attractive as a CCU process.

### *3.2. Algae*

Altogether, an algae-based bio-refinery as shown in Figure 2 consists of multiple units for algae cultivation, harvesting and drying, lipid extraction, remnant treatment (anaerobic digestion), and biogas utilization (power generation) [10]. The biomass residue that remains after extraction of oil can be used as high-protein animal feed (other products). However, the majority of algal biomass residue undergoes anaerobic digestion to produce biogas [19].

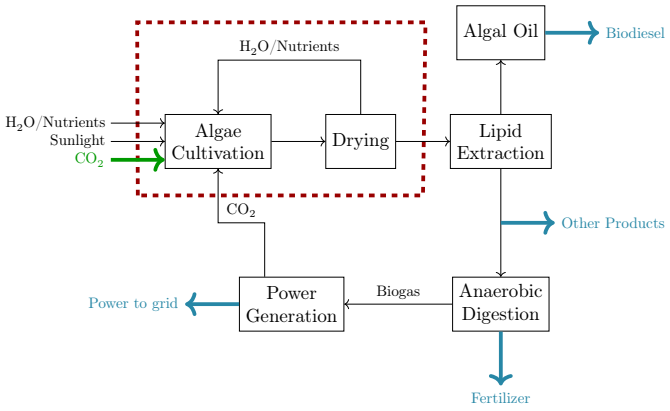


Figure 2: Algae Processing [19]

For the purpose of $CO_2$ utilization, only the production of biomass is considered (as indicated by the dotted red box in Figure 2). A multitude of problems arise when analyzing the production of algae. First of all, the lipid content and growth of algae are negatively correlated [18], which results in a trade-off between the maximization of both quantities. As best practice, future genetic adjustments of the algae species should have the objective to optimize that correlation for simultaneous optimal growth and lipid production. Another major problem arises with the economic feasibility of the state-of-the-art technologies that are currently considered for bio-refinery approaches. As of right now, no plants utilizing algae are run feasibly at an industrial scale (e.g. Solazyme and Sapphire Energy) [18].

Based on the model presented by Gong et al. [10] a mass balance calculation is developed for the production of algal biomass as visualized in Fig. 3. Their research shows that in terms of cost and efficiency algae cultivation and harvesting in an open raceway pond system is the most feasible application based on the use of the microalgae *Phaeodactylum tricornutum*. The small capital investment, the use of free solar energy, easy maintenance, and lower energy requirements are major advantages of raceway ponds [20]. Nevertheless, the downside to open raceway ponds is their reduced productivity. Compared to closed photo-bioreactors, they are affected by bad weather conditions, and may be easily contaminated by external microbes [10].

As the mature algae from the open pond is considerably dilute, drying is necessary. For that purpose, first a sedimentation basin that is capable of concentrating algae slurry to 1% is implemented (compare Figure 3). Additionally, advanced dehydration technology is required, therefore flotation thickening is conducted as well. Split water from the de-watering section is sent back to the open pond as nutrient [10].

| | Value | Unit |
|---|---|---|
| Total Annual Cost | 36.1 | $10^6$ € $a^{-1}$ |
| Annual Production Cost | 33.7 | $10^6$ € $a^{-1}$ |
| Total Capital Investment | 42.7 | $10^6$ € |
| Revenue | 4.2 | $10^6$ € $a^{-1}$ |
| $CO_2$ Utilization Cost | 590 | € $t_{CO_2}^{-1}$ |

Table 2: Economic Evaluation of Algal Biomass Production

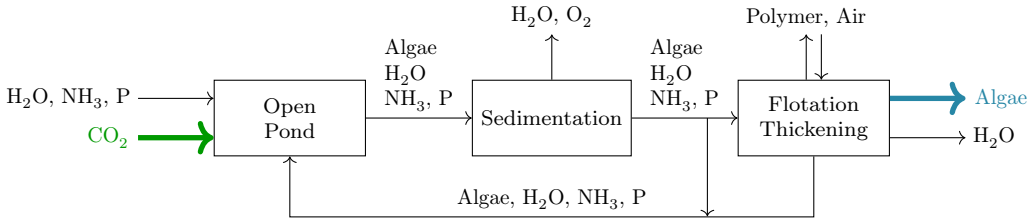


Figure 3: Open Pond Bio Algae Process [10]

Additionally, an economic analysis is conducted based on the work of Yadala et al. [20]. To calculate an acceptable price for algal biomass the approach developed by Chisti [19] is applied. The land cost is set to an average price for agricultural land in Spain (approx. 20 000 €/ha [36]), since the local climate conditions are the most favorable within Europe. To process the intended volume of $CO_2$ an area of approximately 3 $km^2$ is required. The complete economic analysis for algal biomass production is shown in Table 2. The annual production costs (TPC) are affected mostly by the costs for utilities such as water, nutrients, and polymers for flotation. The costs for the total capital investment largely consist of the direct cost, which include site preparation, mixing, $CO_2$ diffusers, harvesting, flocculation, supply system, waste treatment, building and structures, electrical supply and distribution, instrumentation and machinery, and land cost. A revenue is achieved by selling the produced algal biomass. Altogether, a relatively high value for the $CO_2$ utilization cost (590 € $t_{CO_2}^{-1}$) is reached due to the low revenue attained. This is partly caused by the rough estimations and the combination of multiple resources [10, 19, 20, 37], which leads to a significant upwards adjustment. All applied values for parameters can be found in the Supplementary Information (SI) to this report.

Applying the process criteria to algal biomass production results in an average grade of 2.7 as shown in Figure 4. For "technical readiness" the process achieves a grade 3, since prototypes have been developed, but are not at a feasible state of development yet. As the total process can achieve zero greenhouse emission, but only 10% of the injected $CO_2$ is consumed [37], it reaches a grade of 4 for the category "environment". For "market size" it reaches a value of 2 as, the market is growing momentarily, but the demand for biomass is still uncertain.

Altogether, the preliminary results for the production of algal biomass for CCU show that this process is a very environmental friendly approach that has a lot of potential for the future, but needs improvement mainly considering the feasibility of the process.

### *3.3. Chemicals/Fuel Production*

A variety of chemicals is screened with regard to economic potential[3] and stoichiometric $CO_2$ sequestration potential (incorporated $CO_2$), shown in Table 3. Since the production of a lot of chemicals relies on products of other processes, opportunities for mass integration are also considered in the selection.

The most promising products methanol (MeOH), dimethyl ether (DME), and dimethyl carbonate (DMC) are listed along with their various production routes in Table 1. They can further be categorized into bulk chemicals (MeOH, DME), that are produced at low margins in high quantities, and higher value products (DMC).

#### *3.3.1. Methanol (MeOH)*

CCU processes producing methanol are proven to be more $CO_2$ efficient than conventional plants [7] and are likely to have a negative total $CO_2$ impact. In general, methanol serves as a platform chemical, that can be produced in large quantities to incorporate large volumes of $CO_2$ at margins, that are lower compared to DME and DMC [16]. The main chemical derivatives produced from methanol are formaldehyde, acetic acid, methyl tertiary-butyl ether (MTBE), and DME [7]. Due to its excellent combustion properties [38], methanol has great potential as a fuel as it can be blended with gasoline or be used in fuel cells [7]. Additionally, it can serve as a feedstock for the production of diesel fuel replacements.

In total, the market volume is estimated at 61 Mt $a^{-1}$ to 75 Mt $a^{-1}$ [7, 16]. The concept of producing MeOH on basis of $CO_2$ is already applied on industrial scale by the company "Carbon Recycling International" (CRI) in Iceland [39]. This plant has a capacity of 5 million liters per year (since 2015); correlating with an amount of 5.5 thousand tonnes of recycled $CO_2$.

Methanol can be produced via two pathways, that use $CO_2$ as feedstock: via syngas (R5) from combined reforming (R1-3) and via direct hydrogenation of $CO_2$ (R4). The first pathway holds a lot of economic potential, while the second one promises a higher $CO_2$ utilization rate that is 1.38 $t_{CO_2}$ $t_{Product}^{-1}$ compared to 0.3 $t_{CO_2}$ $t_{Product}^{-1}$. Hydrogen for direct hydrogenation of $CO_2$ must be provided to the process in a carbon-free way (e.g. from water electrolysis operated with electricity from renewable energy sources) to reduce the life cycle $CO_2$ emissions [7].

#### *3.3.2. Dimethyl Ether (DME)*

DME is handled as one of the most promising drop-in replacements for conventional fuels [16, 40]. It can be used in transportation as a diesel or gasoline substitute, for electric power generation and in domestic applications in place

[3] Price difference reactants and products.

| Product | Incorporated $CO_2$ [$t_{CO_2}\ t^{-1}_{Product}$] | Plant Size [$kt\ a^{-1}$] | Market Scale [$Mt\ a^{-1}$] |
|---|---|---|---|
| MeOH direct | 1.38 | 375 | 75 |
| MeOH via syngas | 0.3 | 820 | |
| DME from MeOH | 0.5–1.9 | 600 | 6.3 |
| DME via syngas | 0.5 | 600 | |
| DMC | 1.5 | 100 | 0.24 |

Table 3: $CO_2$ Incorporated and Chemical Markets [16, 17, 46]

of liquefied petroleum gas [41]. Clear advantages of DME over other synthetic fuels are its easy liquefaction, which makes storage and transport simpler, its lack of sulfur and noxious substances, which makes DME a clean fuel [42], and its high compatibility with current diesel engines.

Additionally, a considerable market e.g. as reactant in the dimethyl sulfate production does already exist and is estimated to exceed 6.3 Mt/a [11, 16]. DME can either be synthesised directly from syngas (R7) via combined reforming (R1-3) with $0.5\,t_{CO_2}\ t^{-1}_{Product}$ or indirectly via methanol dehydration (R6) and thus incorporate $0.5\,t_{CO_2}\ t^{-1}_{Product}$ to $1.9\,t_{CO_2}\ t^{-1}_{Product}$ depending on the methanol source.

### *3.3.3. Dimethyl Carbonate (DMC)*

The comparably small DMC market (24 Mt/a) is expected to expand in the coming years [43], as DMC's properties as an unregulated solvent [44], its ability to replace MTBE as anti-knocking agent and its increasing usage as reactant for poly carbonate production [45], have sparked interest in the industry. Two different candidates, which have the potential to become a novel and sustainable route for the synthesis of DMC in large scale production, are looked into: The direct carbonylation of methanol is the simplest option but currently achieves only low yields [43]. In accordance with Kongpanna et al. [12] and Santos et al. [45] the transesterification of ethylene carbonate (EC) produced from ethylene oxide (EO) and $CO_2$ (R8) is selected as the most promising candidate due to the high productivity and selectivity for DMC. It incorporates $1.5\,t_{CO_2}\ t^{-1}_{Product}$ and produces ethylene glycol (EG) as a high-value by-product.

### *3.3.4. Evaluation*

Production of MeOH via combined reforming or $CO_2$ hydrogenation, and production of DME via combined reforming or methanol dehydration do not introduce new hazards over conventional processes. The production of DMC via transesterification of ethylene carbonate eliminates phosgene, that is present in conventional processes. These chemicals are thus graded 3, 3, and 4 respectively for MeOH, DME, and DMC in the category "environment".

Market sizes are stated in Table 3. They are mapped to grades of 4, 3 and 2 corresponding to MeOH, DME, and DMC once again.

Technical readiness has been discussed in sections 3.3.1, 3.3.2 and 3.3.3. The routes' average grades are therefore 4 for MeOH, 3 for DME, and 3 for DMC as well. The detailed scores of the different chemicals are visualized in Figure 4.

### *3.4. Comparison of Processes*

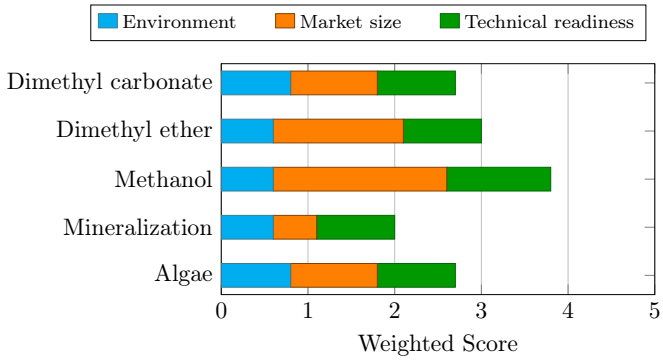


Figure 4: Comparison of Different CCU Processes

Figure 4 shows the overall weighted scores of all CCU processes considered. Clearly, mineralization with a total score of 2 falls behind compared to the other processes. Furthermore, the algal biomass production process with a total score of 2.7 stands a good chance for a continuing more detailed analysis but can not compete with the chemical processes (average total score 3.1) yet. This is owed mostly to the increased market size inhered by the chemicals, most notably for MeOH.

In conclusion, the weighted evaluation of processes indicates that the production of novel chemicals or implementation of new synthesis routes is the most promising CCU method. This production route is thus further studied and shall be analysed in the form of a superstructure optimization.

## 4. Superstructure Formulation

Different process designs for CCU have been studied intensively over the last decade. However, the combination of chemical production processes on the level of complete process design rather than reaction networks has not been addressed very frequently. In fact, this approach enables a more detailed economic evaluation. Since often major expenses arise from compression stages and thermal separation units [38, 45], decisive drawbacks concerning the technical implementation on production scale can be revealed. Moreover, indirect $CO_2$ emissions due to processing can be quantified with higher accuracy, allowing for a fair comparison of process alternatives. Since indirect $CO_2$ emissions might exceed the amount of $CO_2$ which is directly utilized, the integration of processes in terms of mass and energy can reduce this major weak point of stand-alone process designs, increase their overall profitability and improve the environmental impact.

In the following different process alternatives for the proposed chemicals are introduced. Based on that, a superstructure is derived by mass and energy integration of the different processes. Within the purpose of energy integration a combustion unit to utilize the residual flammable components of the purge streams and organic Rankine cycles to recover excess waste heat at low temperature levels are introduced and discussed in section 4.1.5 and 4.1.6. The considered options for integration are outlined and thus need to be evaluated. The decision problem is solved applying superstructure optimization which enables the simultaneous evaluation of different process alternatives as well as their combinations. Accordingly, integer $\mathbf{y}$ and continuous variables $\mathbf{x}$ are assigned to their respective process units and configurations. These are listed in Table 4 along with the description of their physical meaning. Generally, the integer variables $\mathbf{y}$ describe the flowsheet topology whereas the continuous variables $\mathbf{x}$ denote key operating conditions of the processes. Following this path, non-intuitive connectivities, which exhibit synergetic potential, can be obtained.

### *4.1. Process Alternatives*

Several process designs implement the production routes of MeOH, DME and DMC mentioned previously (table 1). In this section, these design options are discussed in further detail for each chemical and production route. Each of them is implemented in the Aspen Plus process modelling software with NRTL-RK as the default property data model. Process flowsheets for each section can be found in the SI of this report.

#### *4.1.1. Syngas Production via Combined Reforming*

Combined reforming (R1-R3) is applied to incorporate $CO_2$ in the production of syngas for a specified composition for synthesis of DME and MeOH respectively. First SMR and hydrocarbon cracking is performed in a prereformer unit (RGibbs) operating at $T = 550\,°C$ and $p = 6\,bar$. In the next step, the main reformer unit (RGibbs) further converts the residual $CH_4$ with $CO_2$ to syngas in a DMR process at approximately $T = 900\,°C$ ($x_2$) and $p = 6\,bar$ [46]. The temperature of the reformer plays a major role for the energy consumption. Therefore, the trade-off between high yield of syngas (high temperature) and low heat requirement (low temperature) is taken into consideration in the optimization.

#### *4.1.2. Methanol*

As stated previously, two different routes for the production of MeOH are taken into consideration ($y_1$). Despite the different reactants both employ similar operation steps. At first, cost intensive compression stages prepare the feed streams followed by the reaction at high pressure and temperature. The reactors' pressure is optimized to take investment cost and energy requirement of the compression stage as well as the yield into account ($x_4$, $x_6$). Different compositions of unreacted gases ($H_2$, CO, $CO_2$) are further separated with flash units at different pressure levels and recycled to the reactor inlet ($x_7$) or to the reforming unit ($y_9$). Optionally, the purge can be used in the combustion unit for supplying additional high temperature heat to the process ($y_2$), which saves $CO_2$ emissions by reducing the amount of natural gas needed. Finally, the separation of water from the process is carried out in a distillation column. Here, in addition to the base design, vapor recompression at the top of the column to supply heat for the reboiler is considered as an option ($y_{10}$, $y_{12}$).

However, the two methanol synthesis routes differ distinctly in the choice of reactors. As proposed by Van-Dal et al. [38], the core of the direct hydrogenation of $CO_2$ to MeOH is an adiabatic fixed-bed reactor operating at $T = 210\,°C$ and approximately $p = 78\,bar$ ($x_6$). The reactor is modeled as an ideal tube-bundle plug-flow reactor with a loading of $44.5\,t_{cat}$, bed voidage of 50 %, tube diameter of 6 cm and length of 10 m. For that, the reformulated kinetic model provided by Van-Dal et al. [38] for an commercially available $Cu/ZnO/Al_2O_3$ catalyst is used. It is possible to utilize the hot outlet stream of the reactor either completely or partially for different energy integration alternatives ($y_{13}$). As suggested by Van-Dal et al. [38] the Soave-Redlich-Kwong equation of state (EOS) with modified Huron-Vidal mixing rules (RKSMHV2) is used to calculate the thermodynamic properties of streams at high pressures ($p > 10\,bar$).

MeOH synthesis from syngas is performed in an isothermal reactor modeled as RGibbs at $T = 250\,°C$ and approximately $p = 81\,bar$ ($x_4$) [46]. For that, combined reforming is required to yield a syngas composition with a molar ratio of $n_{H_2}/(2n_{CO} + 3n_{CO_2}) = 1 \ldots 1.1$ [46]. In both cases formation of by-products such as DME or heavier alcohols is neglected since its impact is assumed small and it would further not preclude the use of the final product as fuel [38].

#### *4.1.3. Dimethyl Ether*

Since the reaction pathways of DME and MeOH are closely related (Table 1), the processes show similarities in their designs. For the direct one-step synthesis of DME, syngas with a molar composition of $H_2/CO = 1.2...1.4$ is fed to a compression stage, mixed with a recycle stream and fed into a single slurry phase reactor modeled as RGibbs at $T = 277\,°C$ and an adjustable pressure of approximately $p = 56\,bar$ ($x_1$) [11]. In the reactor the WGS reaction (R2), the methanol synthesis from syngas (R5) and the methanol dehydration reaction to DME (R6) take place simultaneously. Afterwards, a flash unit is used to separate and recycle unreacted feed gases [11]. The trade-off between lowering the required heat of the reformer and the yield of DME is considered in the amount of recycle to be purged ($x_3$). To provide high temperature heat the combustion unit ($y_2$) needs to be active where the purge is utilized. If the combustion unit is inactive, $x_3$ is expected to meet the lower bound. The purification of the product DME and the

| Variables | Description | Lower Bound | Upper Bound |
|---|---|---|---|
| Integer | | | |
| $y_1$ | DME-Syn, MeOH-Syn or MeOH-Dir active | 0 | 2 |
| $y_2$ | Combustion Unit active | 0 | 1 |
| $y_3$ | DMC active | 0 | 1 |
| $y_4$ | ORC-C active | 0 | 1 |
| $y_5$ | ORC-H active | 0 | 1 |
| $y_6$ | Scale-up of DMC production by buying MeOH | 0 | 1 |
| $y_7$ | Vapor recompression in DMC active | 0 | 1 |
| $y_8$ | DME from MeOH active | 0 | 1 |
| $y_9$ | Recycle of MeOH-Dir Reactor to Reforming Unit active | 0 | 1 |
| $y_{10}$ | Vapor recompression in MeOH-Syn / MeOH-Dir active | 0 | 1 |
| $y_{11}$ | Stream Split after Reactor in MeOH-dir active | 0 | 1 |
| $y_{12}$ | Heat integration: compression stage intercooling with MeOH-$H_2O$ column preheater and ORC-C or only ORC-H active | 0 | 1 |
| $y_{13}$ | Heat integration: MeOH-Dir Reactor outlet stream with DMC, ORC-H or MeOH-$H_2O$ column active | 0 | 2 |
| $y_{14}$ | Heat integration: MeOH-Syn Reactor with DMC, DME or ORC-H active | 0 | 2 |
| Continuous | | | |
| $x_1$ | Pressure DME-Syn Reactor | 50 bar | 60 bar |
| $x_2$ | Temperature Reformer | 850 °C | 950 °C |
| $x_3$ | Purge to Combustion Unit (DME-Syn) | 5 % | 15 % |
| $x_4$ | Pressure MeOH-Syn Reactor | 70 bar | 81 bar |
| $x_5$ | Purge to Combustion Unit (MeOH-Syn) | 3 % | 15 % |
| $x_6$ | Pressure MeOH-Dir Reactor | 70 bar | 80 bar |
| $x_7$ | Purge to Combustion Unit (MeOH-Dir) | 3 % | 15 % |

Table 4: Binary and Continuous Variables

by-product MeOH is realized with three sequential distillation columns; a first column to separate and recycle the residual $CO_2$, a second to purify DME and a third column to separate the residual MeOH-water mixture for further processing.

Traditionally, a two-step route producing MeOH and DME in separate reactors (R6) is applied [42]. This process structure opens the possibility to use MeOH from different synthesis routes. It is then further fed into a high pressure isothermal reactor (RGibbs) at $T = 267\,°C$ and $p = 50\,bar$ to form DME (R6) followed by two distillation columns: one for purification of DME and a second one to separate the remaining MeOH-water mixture such that unreacted MeOH can be recycled to the reactor inlet [11].

#### *4.1.4. Dimethyl Carbonate*

Based on findings by Hsu et al. [47], an intensified process design utilizing a reactive distillation column for the reversible reaction of ethylene carbonate (EC) and excess MeOH to DMC and ethylene glycol (EG) is applied. The $CO_2$ is incorporated in a first step of the process where ethylene oxide (EO) and excess $CO_2$ are reacted to EC (RStoich) [48, 49]. Despite the fact that this process alternative has been reported to have the economic potential to compete with the conventional BAYER process [50], a main issue still remains with the economic and especially ecological separation of the azeotropic pair MeOH and DMC [47–49]. Hsu et al. [47] have found an economically viable option that includes an extractive distillation using aniline as a heavy-entrainer. However, the consumption of $CO_2$ can be exceeded by $CO_2$ emissions due to high energy requirements, which gives rise to potential benefit of energy integration with other processes [49].

UNIQUAC-RK property method is selected to simulate liquid and vapor phase behavior, since these are used in the extractive distillation design by Hsu et al. [47]. The model is further extended by the following units: a compression stage and a pump to achieve the required pressure of 40 bar [48] for the reaction of EO and $CO_2$ to EC, a flash unit to purge the residual $CO_2$ from up-stream processes after the recovery of MeOH, the option to use vapor recompression at the reactive distillation column ($y_7$) and an additional distillation column for the purification of EG.

#### *4.1.5. Combustion Unit*

Since process sections may require heat at elevated temperature levels such as the reforming units, the superstructure is extended by a combustion unit (cf. Figure 6). The residual syngas and other flammable components from purges of different processes are fed to the combustion unit to provide heat at the increased temperature level of 1000 °C. That way, the overall process becomes more energy efficient and indirect $CO_2$ emissions are mitigated, since no excess syngas is wasted and less natural gas is

| Working Fluid | Pressure [bar] | Temperature [°C] | Efficiency [%] |
|---|---|---|---|
| R-274fa (ORC-C) | 1.3 – 3.4 | 21.5 – 75 | 6.2 |
| Pentane (ORC-H) | 0.6 – 5.4 | 21.9 – 150 | 14.9 |

Table 5: Properties of the Employed ORCs

required to supply high temperature heat. Further information and a flowsheet can be taken from SI.

#### *4.1.6. Organic Rankine Cycles*

Depending on mass and energy integration of the considered processes, large amounts of excess heat may occur on low temperature levels. For recovery of this waste heat the superstructure is extended by organic Rankine cycles (ORC) in order to also reduce indirect $CO_2$ emissions which arise from electricity production. Hence, two ORCs on different temperature levels, 75 °C (ORC-C) and 150 °C (ORC-H), are employed. The ORCs are assumed to operate with hot cooling water at 80 °C and 155 °C respectively. Working fluids and operating conditions are further chosen such that residual heat of hot cooling water leaving the evaporator of ORC-H can be integrated with ORC-C. Table 5 summarizes further information on the properties of the employed cycles. A flowsheet with additional information can be taken from SI.

As visualized in Figure 6 the ORCs serve as heat sink for the residual waste heat on sufficient temperature levels. In case only ORC-C is active the entire waste heat is utilized here. In case both ORCs are active their integration as mentioned above is considered.

### *4.2. Mass Integration*

A brief overview of the mass integration options between different MeOH, DME and DMC production routes is presented in Figure 5. They are also referred to in Table 4 with their respective variables ($x$, $y$) used in the optimization. Recycle, purge and byproduct streams add further integration options on a smaller scale, that are not displayed, but their proportion is adjusted within the optimization ($x_3$, $x_6$, $x_8$).

$CO_2$ from carbon capture (indicated by green arrows) is fed to the combined reformer or to the $CO_2$ hydrogenation ($y_1$). The syngas which is produced by combined reforming is further processed in the DME (syngas) production, giving MeOH as a by-product, or in the MeOH (syngas) production. Unconsumed $CO_2$ is recycled to the respective reactors or can be fed back to the reforming unit.

The production of DME via dehydration of MeOH as well as the DMC synthesis can either be fed with MeOH produced from syngas (MeOH syngas) or direct $CO_2$ hydrogenation (MeOH direct). The DMC process runs on non-converted $CO_2$ from upstream purges and possibly on the byproduct MeOH from the DME (syngas) production. This configuration allows the option to buy additional MeOH to extend the DMC production to its largest scale of 100 kt a$^{-1}$ ($y_6$). However, the option to produce DME with residual MeOH from the DME (syngas) process is excluded.

### *4.3. Energy Integration*

To improve the performance of every stand-alone process as well as the combination of certain process designs, it is crucial to perform energy integration within and among the processes. Figure 6 provides an outline of the most important possibilities for heat integration among the different processes. The categorization of all residual hot and cold streams reveals that there is excess heat from the reactors and their outlet streams in the MeOH and DME processes and that heat is required for all thermal separation units. The decision variables are assigned to the respective processes and heat streams. A "plus"-sign indicates that a heat stream can supply all of the connected heat sinks, whereas a "minus"-sign indicates that only one integration can be chosen.

The considered options for energy integration within the superstructure are listed below. Second law violation is indirectly prevented by provision of conservative bounds on temperature levels of the respective streams. All heat exchangers are specified with a minimum temperature difference of 10 K. For some hot streams multiple integration options exist, that are included in the decision variables $y$ (Table 4).

- **Combined reforming**: The outlet stream of the last reformer stage can be utilized to preheat the inlet streams of both reforming units.
- **MeOH syngas**: The outlet stream of the reactor preheats the inlet stream and either provides the complete heat required in the separation section or supplies the ORC-H, if vapor recompression is active ($y_{10}$). Heat from the reactor can be used in DMC, DME or ORC-H ($y_{14}$).
- **MeOH direct**: Intercooling in the compression stage can be integrated with the preheater of the MeOH-Water separation column and the ORC-C or completely in the ORC-H ($y_{13}$). A fraction of the hot reactor outlet stream can preheat the inlet stream ($y_{11}$). The fraction influences the utilization of the residual heat in the down-stream processes. It either preheats the column and $CO_2$-flash or column, DMC and ORC-H ($y_{13}$).
- **DME syngas**: The heat in the reactor outlet stream can preheat the inlet stream. Heat from the reactor can be used in the reboilers of all columns.
- **DME (MeOH)**: Heat from the reactor and in the outlet stream can preheat the inlet stream and the

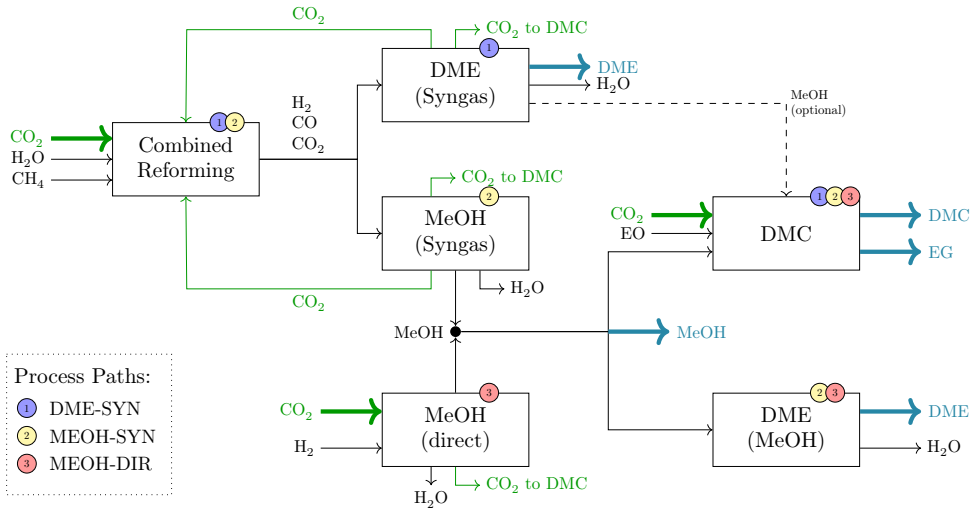


Figure 5: Mass Integration of MeOH, DME and DMC Processes

recycle stream. Heat in the outlet stream of the reactor and the bottom stream of first column can be used to reboil the second column.

- **DMC**: Vapor recompression can be utilized for the reactive distillation ($y_7$) or heat integration from an up-stream process. Residual heat from the compression stage and the EC reactor as well as from the aniline recovery column can heat the flash unit and the streams of EC and MeOH before entering the reactive distillation column.

### *4.4. Modified Superstructure Formulation*

A preliminary analysis of the proposed superstructure reveals that neither heat nor mass is integrated between three main process paths of the superstructure:

- **DME-Syn** using the DME syngas process and the option for further processing of the residual MeOH and $CO_2$ to DMC,
- **MeOH-Syn** including the MeOH syngas process with downstream DME and/or DMC synthesis,
- and **MeOH-Dir** including downstream processing to DME and/or DMC.

Also in a real life application, building multiple plants is unfavorable to a single one due to the economy of scale. Therefore, options that simultaneously consider more than one main process, i.e. MeOH syngas, MeOH direct and DME syngas, as active are omitted. Accordingly, for computation the superstructure is decoupled into the three main paths which is explained in detail in Section 5. With the division into three independent main process paths a reasonable basis for comparison is generated.

## 5. Optimization Problem and Solution Strategy

When designing sustainable processes at least two central aspects have to be taken into consideration – environmental impact and economic feasibility. In certain regions these objectives can be expected to conflict when optimized [22]. Thus, in this work multi-objective superstructure optimization is applied in order to assess the trade-off and find an overall optimal sustainable process.

Environmental impact is optimized by minimization of net $CO_2$ emissions accounting for both direct and indirect emissions (cf. Eq. (1)).

$$\mathrm{CO}_2^{net} = \mathrm{CO}_2^{out} - \mathrm{CO}_2^{in} + f_{el}P_{el} + f_{hs}Q_{hs} + \mathrm{CO}_2^{ref} \quad (1)$$

The terms $f_{el}P_{el}$ and $f_{hs}Q_{hs}$ account for indirect $CO_2$ emissions related to the generation of required electricity ($P_{el}$) and steam ($Q_{hs}$) respectively. High temperature heat required for reforming ($Q_{ref}$) is provided by combustion of methane. The resulting indirect $CO_2$ emissions ($\mathrm{CO_2}^{\mathrm{ref}}$) can thus be calculated according to Eq. (2).

$$\mathrm{CO}_2^{ref} = \frac{Q_{ref}}{LHV_{CH_4}} \frac{M_{\mathrm{CO}_2}}{M_{CH_4}} \quad (2)$$

Economic aspects are translated into total annualized profit as performance indicator. Profit is given by the sum of revenues (REV) and total annualized cost (TAC):

$$\text{Profit} = \text{REV} - \text{TAC}. \quad (3)$$

The TAC include expenses for raw material ($\mathrm{E}_{RM}$), utility costs (AUC) and annualized investment costs (AIC) for an assumed plant life span of 25 years and interest rate of 15 %.

$$\text{TAC} = \text{AIC} + \mathrm{E}_{RM} + \text{AUC} \quad (4)$$

$$\text{AIC} = \frac{i(1+i)^n}{(1+i)^n - 1} \cdot \text{TIC} \quad (5)$$

Investment costs (TIC) are estimated based on Guthrie's modular method. Parameters used in the economic and environmental evaluation are summarized in Table 6. The resultant bi-objective mixed integer nonlinear programming

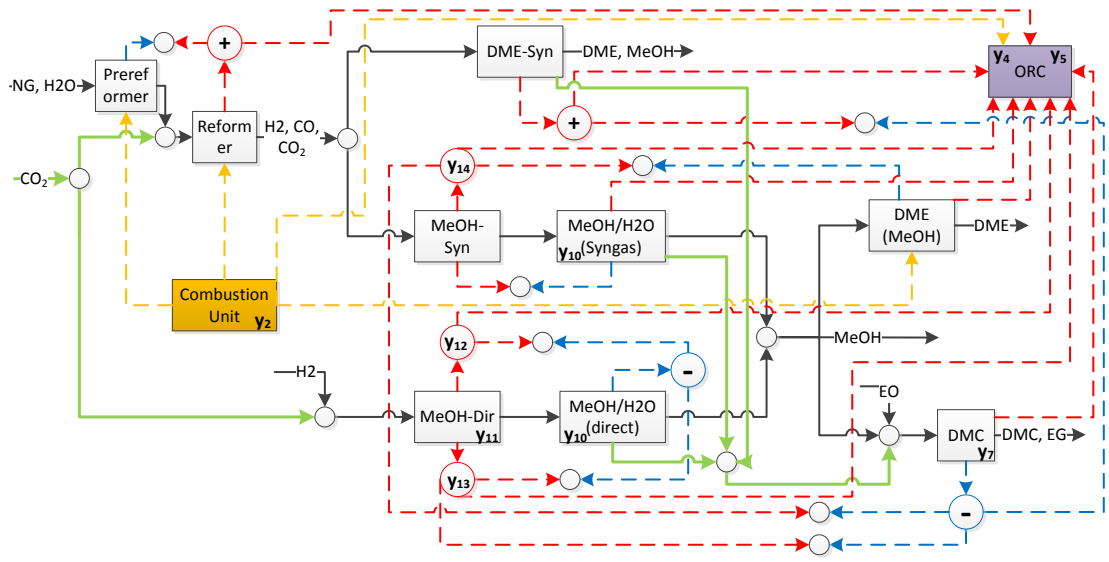


Figure 6: Heat Integration of Processes; green lines indicate $CO_2$ flows, black lines indicate general mass flow, dotted red lines indicate hot streams, dotted blue lines indicate cold streams, dotted yellow lines indicate high temperature heat streams from the Combustion Unit

| Parameter | Description | Value | Unit | Source |
|---|---|---|---|---|
| $f_{el}$ | indirect $CO_2$ emission associated with electricity generation | 0.508 | $t_{CO_2}\,MWh^{-1}$ | [51] |
| $f_{hs}$ | indirect $CO_2$ emissions associated with steam generation | 0.072 | $t_{CO_2}\,GJ^{-1}$ | [51] |
| $i$ | Interest rate | 15 | % | |
| $n$ | Plant life span | 25 | a | |
| $T_{eff}$ | Operating time per year | 8160 | h | |
| $LHV^{L}_{CH_4}$ | Lower heating value of methane | 50013 | $kJ\,kg^{-1}$ | [29] |
| $c_{cw}$ | Cost cooling water | 0.001 | $€\,t^{-1}$ | [52] |
| $c_{hp}$ | Cost high pressure steam (101 bar) | 7.90 | $€\,t^{-1}$ | [53] |
| $c_{mp}$ | Cost medium pressure steam (15 bar) | 6.90 | $€\,t^{-1}$ | [53] |
| $c_{lp}$ | Cost low pressure steam (3 bar) | 6.20 | $€\,t^{-1}$ | [53] |
| $c_{el}$ | Cost electricity | 0.04 | $€\,kWh^{-1}$ | [52] |
| $c_{NG}$ | Cost natural gas | 0.14 | $€\,kg^{-1}$ | [30] |
| $c_{H_2}$ | Cost hydrogen from Biomass gasification (?) | 2.09 | $€\,kg^{-1}$ | [54] |
| $c_{CO_2}$ | Price of $CO_2$ estimated by capture cost | 43.6 | $€\,t^{-1}$ | [27] |

Table 6: Parameters for Economical and Environmental Evaluation

problem (MINLP), stated in (6), is solved using the $\epsilon$-constraint method.

$$\begin{aligned} &\min_{x,y} \quad (-\text{Profit}, \text{CO}_2^{net}) \\ &\text{s.t.} \\ &\left.\begin{aligned} h(x,y) &= 0 \\ g(x,y) &\leq 0 \end{aligned}\right\} \text{Model \& Design Specs} \end{aligned} \tag{6}$$

The flowsheet model of the superstructure is implemented in AspenPlus and additional constraints are considered as design specs. This way, the optimization can be conducted in a reduced space corresponding to the degrees of freedom of the superstructure. Further, due to the complex, non-convex and nonlinear equations which constitute the underlying mathematical model of the flowsheet, the MINLP is solved as black box optimization problem according to the procedure presented by Lee et al. [27]. Hence, the model equations are solved in AspenPlus while the optimization is conducted externally using the genetic algorithm (GA) implemented in MATLAB. In this work a population size of 50, cross-over fraction of 0.8, elite count of 1, Gaussian mutation and stochastic uniform selection is used. As termination criteria 7 consecutive stall generations and a maximum number of 50 populations are specified. As suggested in Section 4.4, the MINLP stated in (6) is further simplified by elimination of the integer variable $y_1$. Instead, the problem is solved by enumeration of three independent MINLPs corresponding to each value of $y_1$. For example $y_1 \neq 0$, i.e. the DME-Syn process path is inactive, implies that all decisions regarding the topology of this process path are irrelevant for the overall process performance. In consequence a majority of the generally possible integer variable combinations of the MINLP stated in (6) yields equivalent solutions. The overall number of possible combinations of all integer variables of Table 4 is 55 296. However, by enumeration of $y_1$

it is reduced to 2368 from which candidate solutions are generated by the GA. Thus, the enumeration is expected to yield an increase of computational efficiency considering the solution method applied. An additional advantage is the enabling of parallelization of calculations.

In a final step, the optimal process based on the Pareto front can be chosen by a decision maker taking different circumstances (e.g. different magnitude of carbon tax associated to the mass of $CO_2$) for production into account.

## 6. Discussion of Results

The computed Pareto fronts for each main process path as well as the separately obtained results from the simplified evaluation in Section 3 for the production of algal biomass and mineralization are visualized in Figure 7. Processes that meet the overall goal of both positive $CO_2$ consumption and a positive profitability (including the $CO_2$ capture) are located in the 1$^{st}$ quadrant. As estimated, the production of algal biomass from $CO_2$ is not profitable ($-36.1\,\mathrm{Mio}\,€\,a^{-1}$). This is due to the very inefficient use of the captured $CO_2$ ($60\,kt_{CO_2}\,a^{-1}$ equivalent to 10 % utilization) and high capital and operating expenses. The ecological potential of mineralization is considerably larger ($300\,kt_{CO_2}\,a^{-1}$) while the implementation of this process is less favourable in terms of costs ($-53.7\,\mathrm{Mio}\,€\,a^{-1}$).

Among the different chemical production processes (MeOH-Dir, MeOH-Syn, DME-Syn) including energy integration, wide-ranging trade-offs between net $CO_2$ consumption and profitability can be reached. The Pareto optimal points (Figure 7) differ mainly in their respective flowsheet topologies.

The processes optimized for maximum $CO_2$ consumption (MS4, MD4, and D3) all share specific characteristics. It is always favourable to recover waste heat using both ORC temperature levels. However, direct heat integration between processes is still favored and therefore only residual heat is utilized by the ORCs. Additionally, the DMC production is operated at the largest scale within each production pathway increasing the direct $CO_2$ consumption. The reformer temperature ($x_2$) is at its lower bound when net $CO_2$ consumption is maximized and at its upper bound for maximum profit. Conveniently, these operating points coincide with minimum heat requirement and maximum yield of the reforming step, respectively.

Further, the optimization of each synthesis path with respect to profit (MD1, MS1, and D1) results in the production of DME from MeOH, or the combined production of DME directly from syngas and DMC from the residual MeOH byproduct. In the most economical configurations neither ORCs nor vapor recompression are active.

In general, it can be concluded that process configurations based on the processing of syngas from combined reforming (MeOH-Syn and DME-Syn) are by far the most profitable. However, due to indirect $CO_2$ emissions caused by the high energy demand of reforming, the overall net $CO_2$ consumption is negative. Nonetheless, these processes still yield an advantageous environmental impact over conventional production of DME and MeOH via SMR. Net $CO_2$ emissions range from 0.12 (D3) to $0.39\,t_{CO_2}\,t_{MeOH}^{-1}$ (MS1). Thus, the $CO_2$ emission of conventional MeOH production in western Europe ($0.76\,t_{CO_2}\,t_{MeOH}^{-1}$ [51]) can be reduced by up to 84 %. In that regard, especially the one-step synthesis of DME from syngas is favored over the two-step production via dehydration of MeOH. Hence, processes based on combined reforming yield an interesting trade-off in short-term perspective. To reduce the amount of natural gas which is used to heat the reformer the combustion unit is always active in these processes. This leads to both, decreased indirect $CO_2$ emissions and lower costs, and is therefore favored irrespective of the objective. Despite the combustion unit being active, however, the purge is minimized for all Pareto optimal configurations. The process configurations based on MeOH production from syngas and its dehydration to DME exhibits the largest economic potential (MS1 and MS2). However, a significant amount of net $CO_2$ emissions (up to 40 %) can be mitigated by waste heat recovery utilizing ORC-H (MS2, MS3) and ORC-C (MS3) as well as integration of DMC production (MS3) with reasonable loss of profit (up to 12 %).

The range of profits for DME-Syn (D1 – D3) of 382−394 $\mathrm{Mio}\,€\,a^{-1}$ is small compared to the possible error margin of about 40 % according to the used procedure for preliminary costing [52]. However, the $CO_2$ emission can be halved from point D1 to D3 by optimizing the process with respect to the maximum $CO_2$ consumption without loosing considerable amounts of profit. Due to the high demand of electricity for the compression stage the reactor pressure increases from 50 bar for maximum $CO_2$ consumption (D3) to 60 bar for maximum profit (D1). The reactor pressure of D2 is about 57 bar.

In summary, these processes can reduce $CO_2$ emissions, when being applied to existing markets and replacing conventional processes. The only process options capable of positive net $CO_2$ consumption are based on direct hydrogenation of $CO_2$ to MeOH (MeOH-Dir). However, these superstructure configurations yield significantly smaller profit mainly due to high cost associated with carbon-neutral hydrogen.

The MeOH-Dir path which is optimized with respect to its profitability (MD1) and the configuration MD2 consume more than $400\,kt_{CO_2}\,a^{-1}$ and are at least cost-neutral, i.e. they cover the cost for $CO_2$ capture. It also has to be noted that the direct hydrogenation of $CO_2$ gives rise to more efficient $CO_2$ utilization compared to combined reforming since for utilization of the same amount of $CO_2$ (cf. reference case) less than 50 % ($375\,kt\,a^{-1}$) of MeOH needs to be produced. Thus, a higher overall potential amount of $CO_2$ can be incorporated. This yields the short-term potential to compete with CCS and therefore the processes are reviewed in more detail.

The process flowsheet associated with point MD1 is

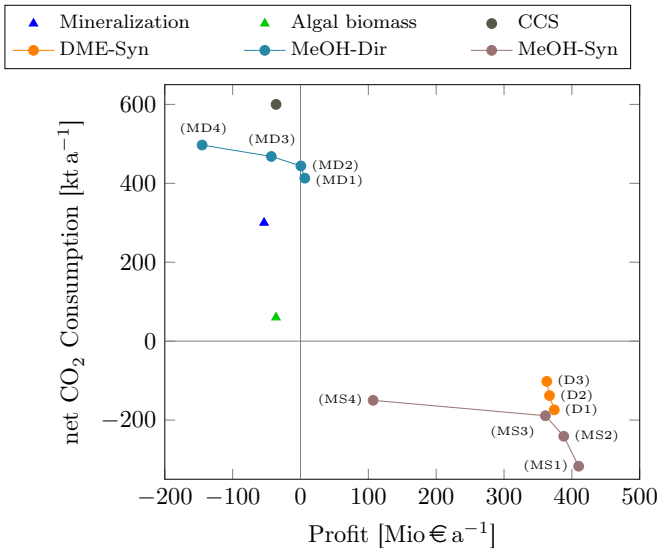


Figure 7: Pareto Optimal Results of Superstructure Optimization; profit includes carbon capture costs.

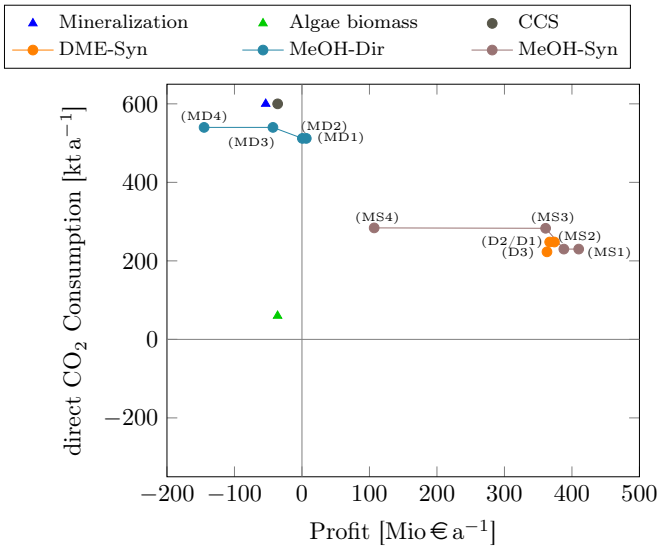


Figure 8: Direct $CO_2$ consumption of Pareto optimal processes with respect to net $CO_2$ consumption and profit.

shown in Figure 9. The process includes an active stream split after the reactor to supply heat for the reboiler of the distillation column (B33) and the low pressure flash unit (B31) as well as for the preheating of the reactor inlet stream. At the optimal point the reactor is operated at 73.3 bar. Furthermore, the purge to the combustion unit is at its lower bound ($x_7 = 0.03$). The combustion unit (indicated blue in Figure 9), however, is active and still able to supply the entire heat required in the MeOH dehydration to DME process (indicated orange in Figure 9). Both processes only differ with respect to waste heat recovery. Whereas the most economical process (MD1) does not utilize any waste heat, process MD2 recovers high temperature waste heat utilizing ORC-H. The main assumption behind this process is the carbon free production of $H_2$ from central biomass gasification, which results in a large overall $CO_2$ consumption. It is reasonable that the additional application of ORCs and production of comparably small amounts of DMC instead of DME would not lead to a significantly larger amount of net $CO_2$ consumed. Moreover, the optimization in terms of $CO_2$ consumption results in enormous profit reduction. This is mainly due to the high investment cost associated with ORCs, and the production of MeOH with much lower margin compared to DME. The configurations of all displayed points are summarized in detail in the SI.

Figure 8 illustrates the direct $CO_2$ consumption neglecting indirect emissions for the respective processes also shown in Figure 7. As mentioned before, the environmental performance of processes based on combined reforming is strongly affected by indirect $CO_2$ emissions. However, it should also be kept in mind that provision of low cost carbon-free energy would likely result in lower cost for carbon-free $H_2$ and thus benefit direct hydrogenation of $CO_2$ economically. Hence, from a long-term perspective it can be concluded that provision of renewable carbon-free energy at low cost is of great importance for these CCU processes to emerge.

### *6.1. Safety and Social Impact*

In addition to financial and ecological aspects, safety, controllability and social impact of the proposed process shall be reviewed to allow a fair comparison to other proposals. One essential aspect in the evaluation of CCU processes is the acceptance among the population, as this is one of the obstacles, that CCS currently struggles to overcome [5, 6]. Other than that, the implementation of $CO_2$ in the production process of common chemicals have additional advantages. Hydrogenation of $CO_2$ uses equipment that is common in the chemical industry and has been proven over decades [21]. The risk for humans can thus be minimized to that of a conventional chemical plant; their acceptance can thus be expected. Likewise, the safety of the process can be guaranteed and controllability expected, as industrial safety standards are naturally required.

## 7. Conclusion and Outlook

Different options for CCU including mineralization, algal biomass production and production of chemicals from a $CO_2$ feedstock have been compared. The comparison is based on utilization of 20 % of the $CO_2$ emissions of 500 $MW_{el}$ power plant as a reference situation. A preliminary screening with regard to technical, economic and environmental criteria revealed that the production of chemicals such as MeOH, DME, and DMC appear to be the most promising options.

The production of MeOH and DME via combined reforming, direct hydrogenation of $CO_2$, dehydration of MeOH to DME as well as the EO-route for DMC production

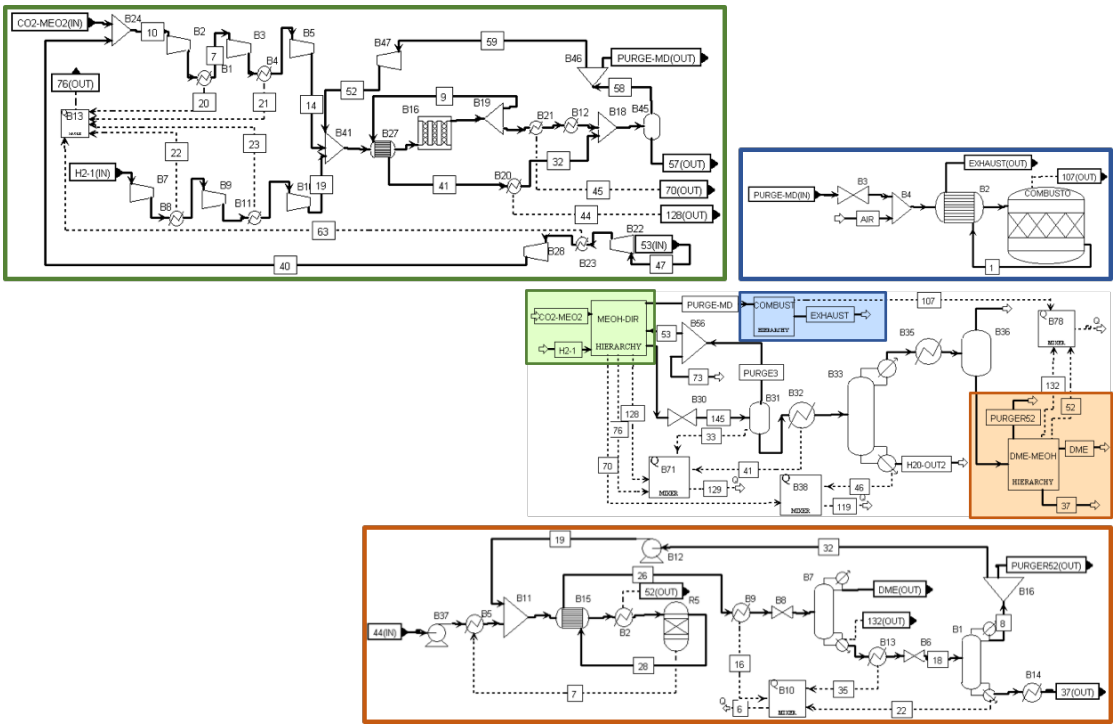


Figure 9: Process Flowsheet for MeOH-Dir Optimized with Respect to Profitability; green marks the direct generation of MeOH, orange marks the MeOH dehydration to DME process, blue marks the combustion unit.

have been addressed in more detail. A superstructure of energy and mass integration of these process pathways was developed and extended by options for energy integration utilizing waste heat recovery by ORCs and a combustion unit.

In order to assess the trade-off between economic and environmental aspects for the entire range of circumstances, multi-objective superstructure optimization was applied. For that purpose, economic and environmental aspects were translated into profit and net $CO_2$ emissions as performance indicators.

The results indicate that from a short-term perspective only the direct hydrogenation of $CO_2$ with carbon-neutral $H_2$ and sequential dehydration of MeOH to DME is capable of positive net $CO_2$ consumption while covering the cost for carbon capture and thus can compete with CCS. In the vicinity of profitability, approx. 68 % of the supplied $CO_2$ can be utilized under consideration of indirect $CO_2$ emissions. Also process configurations based on combined reforming exhibit an interesting trade-off as they can undercut the $CO_2$ emissions from conventional production significantly while generating substantial profit. High indirect $CO_2$ emissions due to high energy demand, however, result in an overall negative net $CO_2$ consumption. Here the one-step production of DME from syngas from combined reforming appears more promising with respect to environmental aspects than the two-step production via MeOH dehydration. From a long-term perspective, especially the provision of carbon-free renewable energy is crucial for the considered CCU processes to emerge.

Further research should aim towards identifying possible future scenarios for the development of renewable energy supply in order to assess the long-term perspective in more detail. Also, the scope of the evaluation should be extended to a holistic assessment including the entire life cycle of $CO_2$ accounting for raw material generation and product use in order to avoid pitfalls in the environmental evaluation. Additionally, a sensitivity analysis should be conducted with respect to the most crucial assumptions of this work.

## Supplementary Information is attached

## 8. References


[1] European Comission, 2030 climate & energy framework. URL http://ec.europa.eu/clima/policies/strategies/2030_en

[2] European Comission, Report on review of directive 2009/31/ec on the geological storage of carbon dioxide.

[3] J. Gibbins, H. Chalmers, Carbon capture and storage, Energy Policy 36 (12) (2008) 4317–4322.

[4] R. S. Haszeldine, Carbon capture and storage: how green can black be?, Science 325 (5948) (2009) 1647–1652.

[5] R. Krupp, Geologische Kurzstudie zu den Bedingungen und möglichen Auswirkungen der dauerhaften Lagerung von $CO_2$ im Untergrund, Hg. v. Bund für Umwelt und Naturschutz Deutschland eV (BUND). Berlin.

[6] RWE Innovation, Rwe igcc-ccs project. URL http://www.rwe.com/web/cms/en/2688/rwe/innovation/power-generation/fossil-fired-power-plants/igcc-ccs-power-plant/

[7] M. Pérez-Fortes, J. C. Schöneberger, A. Boulamanti, E. Tzimas, Methanol synthesis using captured $CO_2$ as raw material: techno-economic and environmental assessment, Applied Energy 161 (2016) 718–732.

[8] R. M. Cuéllar-Franca, A. Azapagic, Carbon capture, storage and utilisation technologies: A critical analysis and comparison of their

life cycle environmental impacts, Journal of $CO_2$ Utilization 9 (2015) 82–102.
[9] H. Geerlings, R. Zevenhoven, $CO_2$ mineralization-bridge between storage and utilization of $CO_2$, Annual review of chemical and biomolecular engineering 4 (2013) 103–117.
[10] J. Gong, F. You, Optimal design and synthesis of algal biorefinery processes for biological carbon sequestration and utilization with zero direct greenhouse gas emissions: Minlp model and global optimization algorithm, Industrial & Engineering Chemistry Research 53 (4) (2014) 1563–1579.
[11] L. Tock, M. Gassner, F. Maréchal, Thermochemical production of liquid fuels from biomass: Thermo-economic modeling, process design and process integration analysis, Biomass and Bioenergy 34 (12) (2010) 1838–1854.
[12] P. Kongpanna, V. Pavarajarn, R. Gani, S. Assabumrungrat, Techno-economic evaluation of different $CO_2$-based processes for dimethyl carbonate production, Chemical Engineering Research and Design 93 (2015) 496–510.
[13] A. Sanna, M. R. Hall, M. Maroto-Valer, Post-processing pathways in carbon capture and storage by mineral carbonation (ccsm) towards the introduction of carbon neutral materials, Energy & Environmental Science 5 (7) (2012) 7781–7796.
[14] H. Xie, T. Liu, Z. Hou, Y. Wang, J. Wang, L. Tang, W. Jiang, Y. He, Using electrochemical process to mineralize $CO_2$ and separate $Ca^{2+}/Mg^{2+}$ ions from hard water to produce high value-added carbonates, Environmental Earth Sciences 73 (11) (2015) 6881–6890.
[15] J. Fagerlund, E. Nduagu, I. Romão, R. Zevenhoven, $CO_2$ fixation using magnesium silicate minerals part 1: process description and performance, Energy 41 (1) (2012) 184–191.
[16] C.-H. Huang, C.-S. Tan, A review: $CO_2$ utilization, Aerosol Air Qual. Res 14 (2014) 480–499.
[17] C.-J. Lee, Y. Lim, H. S. Kim, C. Han, Optimal gas-to-liquid product selection from natural gas under uncertain price scenarios, Industrial & Engineering Chemistry Research 48 (2) (2008) 794–800.
[18] T. Zirbs, M. Häcker, Mikroalgen - Energieträger der Zukunft, Seminar Elektrische Systeme (2013) 21–27.
[19] Y. Chisti, Biodiesel from microalgae beats bioethanol, Biotechnology Advances 25 (2007) 294306.
[20] S. Yadala, S. Cremaschi, A dynamic optimization model for designing open-channel raceway ponds for batch production of algal biomass, Processes 4 (2) (2016) 10.
[21] Y. Lim, C.-J. Lee, Y. S. Jeong, I. H. Song, C. J. Lee, C. Han, Optimal design and decision for combined steam reforming process with dry methane reforming to reuse $CO_2$ as a raw material, Industrial & Engineering Chemistry Research 51 (13) (2012) 4982–4989.
[22] I. E. Grossmann, G. Guillén-Gosálbez, Scope for the application of mathematical programming techniques in the synthesis and planning of sustainable processes, Computers & Chemical Engineering 34 (9) (2010) 1365–1376.
[23] S. Höller, P. Viebahn, Assessment of $CO_2$ storage capacity in geological formations of germany and northern europe, Energy Procedia 4 (2011) 4897–4904.
[24] E. T. P. for Zero Emission Fossil Fuel Power Plants (ZEP), The costs of $CO_2$ capture,transport and storage - post-demonstration ccs in the eu.
[25] STEAG GmbH, Kraftwerk Lünen (2016).
URL https://www.steag.com/s-kraftwerke-luenen.html
[26] E. S. Rubin, J. E. Davison, H. J. Herzog, The cost of $CO_2$ capture and storage, International Journal of Greenhouse Gas Control 40 (2015) 378–400.
[27] U. Lee, J. Burre, A. Caspari, J. Kleinekorte, A. Schweidtmann, A. Mitsos, Techno-economic optimization of a green-field post-combustion $CO_2$ capture process using superstructure and rate-based models, Industrial & Engineering Chemistry Research.
[28] H. H. Khoo, P. N. Sharratt, J. Bu, T. Y. Yeo, A. Borgna, J. G. Highfield, T. G. Bjorklof, R. Zevenhoven, Carbon capture and mineralization in singapore: preliminary environmental impacts and costs via lca, Industrial & Engineering Chemistry Research 50 (19) (2011) 11350–11357.
[29] E. Hahne, Technische Thermodynamik: Einführung und Anwendung, Oldenbourg Verlag, 2011.
[30] NASDAQ, Natural gas.
URL http://www.nasdaq.com/markets/natural-gas.aspx?timeframe=6m
[31] Zevenhoven, Romao, Fagerlund, Nduagu, $CO_2$ fixation using magnesium silicate minerals. part 2: Process energy efficiency, Proceedings of ECOS.
[32] I. Romão, L. M. Gando-Ferreira, R. Zevenhoven, Separation and recovery of valuable metals extracted from serpentinite during the production of $Mg(OH)_2$ for $CO_2$ sequestration, Minerals Engineering 77 (2015) 25–33.
[33] N. von der Assen, J. Jung, A. Bardow, Life-cycle assessment of carbon dioxide capture and utilization: avoiding the pitfalls, Energy & Environmental Science 6 (9) (2013) 2721–2734.
[34] I. S. S. Romão, Production of magnesium carbonates from serpentinites for $CO_2$ mineral sequestration-optimisation towards industrial application, Ph.D. thesis, Department of Chemical Engineering, Faculty of Sciences and Technology, University of Coimbra (2015).
[35] I. Romão, M. Eriksson, E. Nduagu, J. Fagerlund, L. Gando-Ferreira, R. Zevenhoven, Carbon dioxide storage by mineralisation applied to a lime kiln, ECOS.
[36] D. Linden, Preise für Ackerland in Europa 2011.
URL http://fachgruppe-obstbau.de/termine_pics/Preise_fuer_Ackerland_in_Europa.pdf
[37] R. Slade, A. Bauen, Micro-algae cultivation for biofuels: Cost, energy balance, environmental impacts and future prospects, Biomass and Bioenergy 53 (2012) 29–38.
[38] É. S. Van-Dal, C. Bouallou, Design and simulation of a methanol production plant from $CO_2$ hydrogenation, Journal of Cleaner Production 57 (2013) 38–45.
[39] Carbon Recycling International, World's largest $CO_2$ methanol plant.
URL http://carbonrecycling.is/george-olah/2016/2/14/worlds-largest-co2-methanol-plant
[40] T. A. Semelsberger, R. L. Borup, H. L. Greene, Dimethyl ether (DME) as an alternative fuel, Journal of Power Sources 156 (2) (2006) 497–511.
[41] International DME Association, Price for DME (2016).
URL www.aboutdme.org
[42] P. L. Spath, D. C. Dayton, Preliminary screening-technical and economic assessment of synthesis gas to fuels and chemicals with emphasis on the potential for biomass-derived syngas, Tech. rep., DTIC Document (2003).
[43] H. Kuenen, H. Mengers, D. Nijmeijer, A. van der Ham, A. Kiss, Techno-economic evaluation of the direct conversion of $CO_2$ to dimethyl carbonate using catalytic membrane reactors, Computers & Chemical Engineering 86 (2016) 136 – 147.
[44] B. Schaffner, F. Schaffner, S. P. Verevkin, A. Borner, Organic carbonates as solvents in synthesis and catalysis, Chemical reviews 110 (8) (2010) 4554–4581.
[45] B. A. Santos, V. M. Silva, J. M. Loureiro, A. E. Rodrigues, Review for the direct synthesis of dimethyl carbonate, ChemBioEng Reviews 1 (5) (2014) 214–229.
[46] C. Zhang, K.-W. Jun, G. Kwak, Y.-J. Lee, H.-G. Park, Efficient utilization of carbon dioxide in a gas-to-methanol process composed of $CO_2$/steam–mixed reforming and methanol synthesis, Journal of $CO_2$ Utilization 16 (2016) 1–7.
[47] K.-Y. Hsu, Y.-C. Hsiao, I.-L. Chien, Design and control of dimethyl carbonate- methanol separation via extractive distillation in the dimethyl carbonate reactive-distillation process, Industrial & Engineering Chemistry Research 49 (2) (2009) 735–749.
[48] L. F. Souza, P. R. Ferreira, J. L. de Medeiros, R. M. Alves, O. Q. Araujo, Production of DMC from $CO_2$ via indirect route: Technical–economical–environmental assessment and analysis, ACS Sustainable Chemistry & Engineering 2 (1) (2013) 62–69.
[49] C. Choomwattana, A. Chaianong, W. Kiatkittipong, P. Kongpanna, A. T. Quitain, S. Assabumrungrat, Process integration of dimethyl carbonate and ethylene glycol production from biomass and heat exchanger network design, Chemical Engineering and Processing: Process Intensification.
[50] P. Kongpanna, D. K. Babi, V. Pavarajarn, S. Assabumrungrat, R. Gani, Systematic methods and tools for design of sustainable chemical processes for $CO_2$ utilization, Computers & Chemical Engineering 87 (2016) 125–144.
[51] M. Pérez-Fortes, E. Tzimas, Techno-economic and environmental evaluation of $CO_2$ utilisation for fuel production: Synthesis of methanol and formic acid, JRC Science for Policy Report.
[52] L. T. Biegler, I. E. Grossmann, A. W. Westerberg, Systematic methods for chemical process design, Prentice Hall, 1997.
[53] R. Smith, P. Varbanov, et al., What's the price of steam?, Chemical engineering progress 101 (7) (2005) 29–33.
[54] M. Ruth, Hydrogen production cost estimate using biomass gasification: Independent review, Tech. rep., National Renewable Energy Laboratory (NREL), Golden, CO. (2011).